

Journal Name

ARTICLE TYPE

Cite this: DOI: 00.0000/xxxxxxxxxx

Bending stiffness of *Candida albicans* hyphae as a proxy of cell wall properties[†]

Elodie Couttenier^{a,b} Sophie Bachellier-Bassi,^b Christophe d'Enfert,^b and Catherine Villard^{*a‡}

Received Date

Accepted Date

DOI: 00.0000/xxxxxxxxxx

Supplementary information

^a Physico-Chimie Curie, Université PSL, CNRS UMR168, F-75005 Paris, France.

^b Institut Pasteur, Université Paris Cité, INRAE, USC2019, Unité Biologie et Pathogénicité Fongiques, F-75015 Paris, France.

[‡] Present address: Laboratoire Interdisciplinaire des Energies de Demain, Université Paris Cité, UMR 8236 CNRS, F-75013, Paris, France

* Corresponding author. E-mail: catherine.villard@u-paris.fr.

1 - Numerical simulations to validate the theoretical model

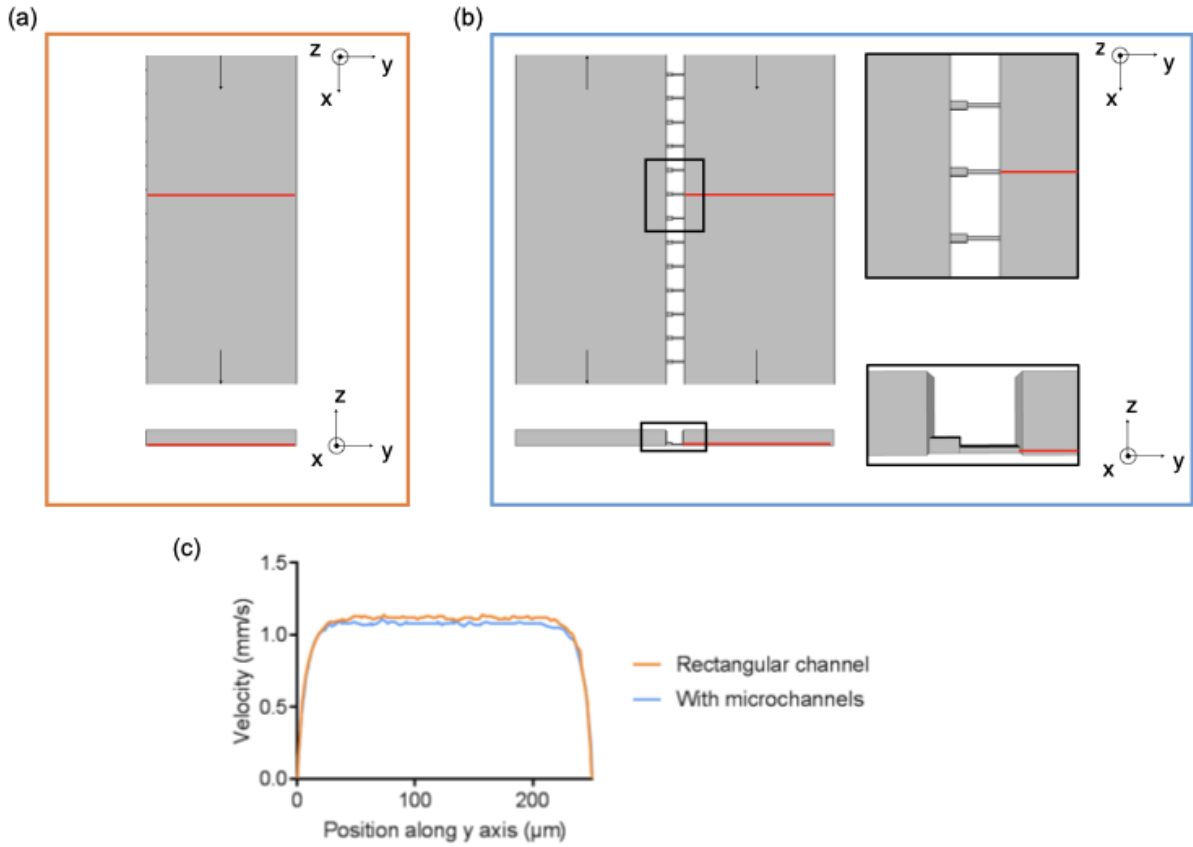


Figure S1 - Numerical simulations with Comsol to study the flow in the bending chamber. Comparison of the flow in a simple rectangular channel (a) and in the bending chamber included in the whole chip, taking into account the presence of microchannels (b). (c) The velocity (mm/s) is plotted along the red line in both situations as a function of y position (μm) close to the hyphae position at a fixed z position ($z = 1 \mu\text{m}$).

2 - Two height microchannels

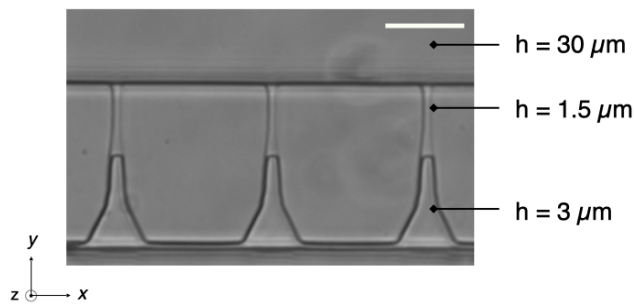


Figure S2 - Phase contrast image of microchannels. The height of each portion is indicated, as well as the height of the bending chamber. Scale bar: $20 \mu\text{m}$.

3 - Influence of the distance between microchannels (filaments) on the measured deflection under flow

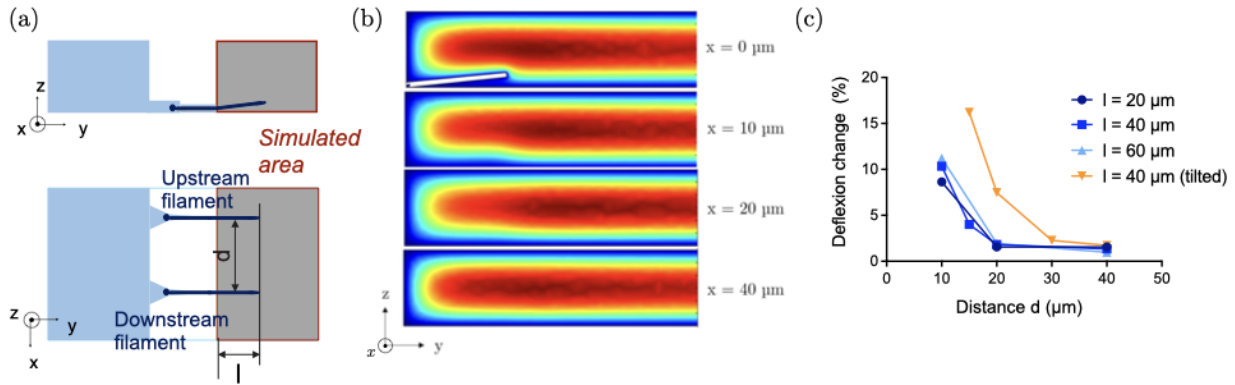


Figure S3 - Optimization of the distance between microchannels along the x axis to minimize the flow perturbation induced by a filament on a second filament located downstream at a distance d . (a) Scheme of our system: cross section (top) and top view (bottom). The area framed in red correspond to the portion of the device modeled using Comsol. We chose to consider the two situations of an upstream filament oriented along the y axis or tilted in the (y,z) plane (only the latter is shown here). The downstream filament is always oriented along the y axis in the absence of flow. Although we consider only hyphae positioned close to the glass surface to assess the bending stiffness, such correctly positioned hyphae may be located downstream of a tilted hypha. This case is thus worth to be examined. (b) Velocity profiles in the bending chamber for increasing distances along the x axis away from a $40 \mu\text{m}$ -long tilted filament located in the (y,z) plane, modeling an hypha non adhering to the surface. The changes in the velocity profile vanished at a distance of $40 \mu\text{m}$ away from the tilted filament. (c) Difference (in percent) in the amplitude of deflection under flow of a filament located downstream another filament as compared to the deflection of an isolated hypha. As expected, this difference in the amplitude of deflection decreases as the distance between the two filaments increases. The length of the filaments (an identical length of the upstream and downstream filaments is considered here) has little influence on the results, while the impact of an inclined upstream filament is greater than that of a filament located on the surface of the substrate. It however vanishes for an inter-filament distance of $40 \mu\text{m}$, in agreement with the velocity profile shown in (b).

4 - Numerical simulations of velocity profiles

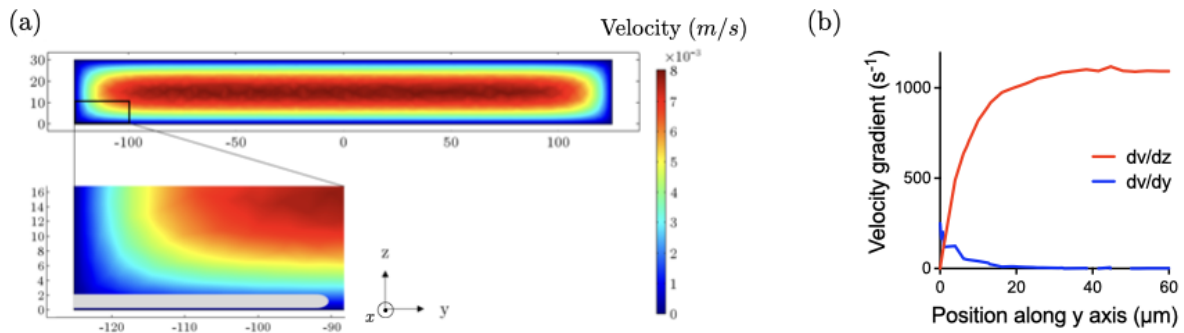


Figure S4 - Flow in the bending chamber: numerical simulations with Comsol. (a) Velocity profile in a rectangular channel of width $L = 250 \mu\text{m}$ and height $h = 30 \mu\text{m}$ for an inlet velocity of 5 mm/sec . The insert shows an enlargement of the area of interest, where the hyphae come out of the microchannel (in light grey). (b) Velocity gradient (in sec^{-1}) dv/dz and dv/dy along the y axis at a height $z = 1 \mu\text{m}$. For filaments whose length ranges from 20 to $50 \mu\text{m}$, gradient along y is negligible compared to the one along z . Moreover, it appears clearly that dv/dz varies as a function of y close to $y = 0$, i.e. at the microchannel exit.

5 - Controls for caspofungin application

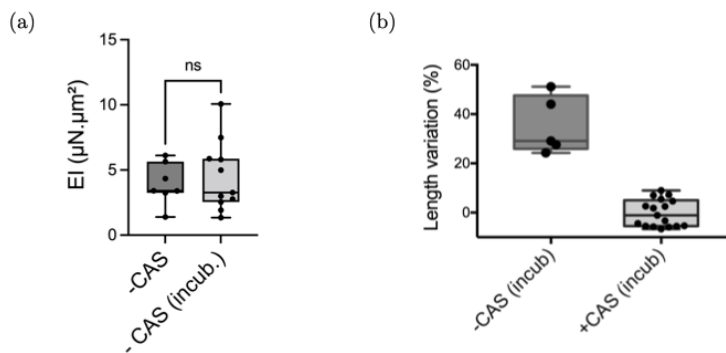


Figure S5 - Influence of the incubation time. (a) Influence of the incubation time on the bending stiffness in the absence of caspofungin. The condition -CAS (incub.) correspond to data collected from hyphae submitted to a 30 min step in the incubator after an initial measurement (-CAS). (b) Influence of a 30 min incubation time on hyphal length with (+CAS) or without (-CAS) casponfungin in the incubation medium. The length variation is expressed as $\frac{L_a - L_b}{L_b}$, with L_b and L_a the lengths before and after the incubation step, respectively.

6 - Paired data associated to bending stiffness measurements

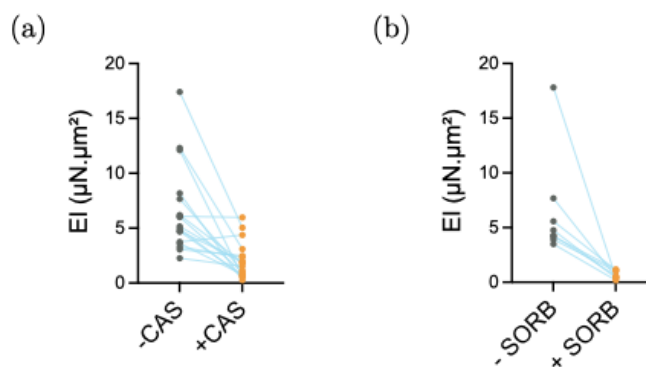


Figure S6 - Distribution of bending stiffness values before and after caspofungine (a) and sorbitol (b) application. Paired data corresponding to figures 4c and 5b right are represented.

7 - Influence of hyphae length on EI

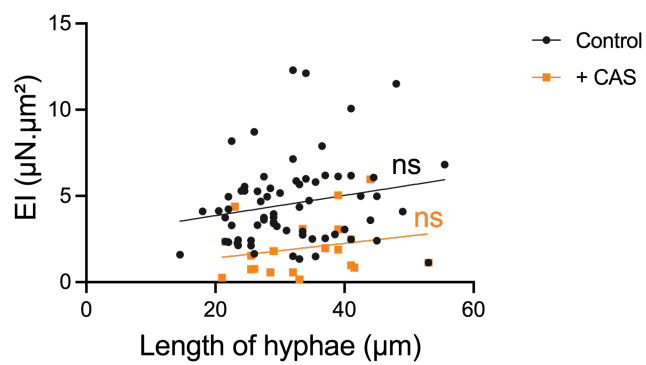


Figure S7 - Bending stiffness as a fonction of hyphal length in SC5314 hyphae without (Control) and after caspofungin application (+CAS). The linear fits show not trend.